Cancer Chemother Pharmacol (1996) 38: 499–507

ORIGINAL ARTICLE

Damayanthi Devineni · Andres Klein-Szanto
James M. Gallo

In vivo microdialysis to characterize drug transport in brain tumors: analysis of methotrexate uptake in rat glioma-2 (RG-2)-Bearing rats

Received: 11 July 1995/Accepted: 1 February 1996

Abstract Brain microdialysis was applied to sample free methotrexate (MTX) concentrations in brain extracellular fluid of normal and RG-2 glioma-bearing rats. All animals received 50 mg/kg of MTX intraarterially following which serial blood and interstitial fluid samples were collected for 3 h and measured for MTX by an HPLC assay. Retrodialysis was used to estimate the in vivo recovery of MTX from brain. A linear two-compartment model was fitted to the plasma MTX concentration-time data in both the normal and RG-2 groups. The mean total body clearance and volume of distribution at steady state of MTX varied from 0.90 ± 0.3 to $0.24 \pm 0.02\,l\,h^{-1}\,kg^{-1}$ ($P < 0.05$) and from 0.58 ± 0.24 to $0.21 \pm 0.16\,l\,kg^{-1}$ ($P < 0.05$) in control and tumor rats, respectively. The significant reductions in clearance and volume of distribution at steady-state were attributed in part to a cachectic state in the RG-2 animals in which total body water was reduced. The mean MTX area under the interstitial fluid concentration-time curve (AUC) was $171.6 \pm 69.14\,\mu g\,min\,ml^{-1}$(control) and $583.5 \pm 296.7\,\mu g\,min\,ml^{-1}$ (brain tumor-bearing rats). The significantly higher AUC values obtained with RG-2 rats compared with control rats may have resulted from high plasma MTX concentrations and a more permeable blood–tumor barrier (BTB). A hybrid physiologically based pharmacokinetic model was used to characterize the mechanisms responsible for the high MTX brain tumor concentrations. In conclusion, a microdialysis technique was successfully utilized to examine the extracellular uptake of MTX in brain. This technique can be a powerful tool to evaluate intracerebral drug kinetics and the delivery of drugs to brain tumors.

D. Devineni · A. Klein-Szanto · J.M. Gallo (✉)
Department of Medical Oncology, Fox Chase Cancer Center,
7701 Burholme Avenue, Philadelphia, PA 19111, USA
Tel. (215) 728–2461; FAX (215) 728–2741

Key words Microdialysis · Pharmacokinetics · Methotrexate · RG-2 glioma

Introduction

The extracellular fluid (ECF) can be viewed as a liquid compartment in which traffic of compounds and the exchange of chemical information between cells take place. It is of considerable importance to be able to monitor changes in the composition of the ECF as well as to measure free concentrations of endogenous and exogenous compounds. Many experimental attempts (e.g. ventricular perfusions, push–pull cannulae and cortical cup perfusions) have been made to monitor the extracellular environment of the intact brain [4]. The ideal method must provide instantaneous and reliable interstitial concentration measurements of a wide variety of substances in discrete brain areas. Furthermore, normal tissue structure and metabolism should be left completely unchanged during the experimental procedure. Noninvasive methods like positron emission tomography (PET) and single photon emission tomography [9, 19], which have been developed to study drug transport, are relatively expensive and difficult to apply in rodent pharmacokinetic studies where a high degree of specificity and sensitivity are required.

Microdialysis is an invasive technique that has been recently developed to obtain representative samples of substances in the ECF from discrete locations in the brain. The advantages of this technique have been reviewed by several authors [4, 24, 40] and validated by comparison with in vivo electrochemical methods and tissue assays [32]. Compared to other in vivo techniques, microdialysis has the advantage of leaving endogenous nutrition and oxygenation as well as synaptic integration and neuronal impulses largely intact. Microdialysis also enables repeated measurements in

conscious animals with minimal damage to brain tissue. This technique has been predominantly used to determine extracellular measurements of endogenous substances [6, 41], and recently it has been extended to the field of pharmacokinetics to determine the concentration of drug in blood [33], liver [48], subcutaneous tissue [26], subcutaneous tumor [29], muscle [29], brain [27, 37, 46] and the vitreous cavity of the eye [3] and to the assessment plasma protein binding [20].

Methotrexate (MTX) is a folic acid antagonist which has been in clinical use for more than four decades. It has been used for the treatment of primary and metastatic brain tumors [1, 15], but its current use is primarily restricted to central nervous system (CNS) lymphomas [10]. MTX has been used in our laboratory as a component in a novel magnetic drug delivery system [14], and in the current investigation served as a model anticancer agent with limited blood–brain barrier (BBB) permeability. The distribution of MTX in the CNS has been investigated. As a weak organic acid, MTX is negatively charged at neutral pH, has limited lipid solubility, and therefore diffuses slowly across physiologic membranes. These properties limit the drug's ability to cross the BBB into the cerebrospinal fluid (CSF) [34] or third-space fluid compartments, such as pleural effusion and ascites [42]. Chatelut et al. [11] reported a mean steady-state CSF/serum MTX concentration ratio of 2.3% in children with brain tumors. Since the composition of CSF is, however, very different from that of brain tissue, and drug concentrations in CSF do not necessarily reflect drug concentrations in brain parenchyma, a direct method to evaluate brain parenchyma drug concentrations would be advantageous. However, to generate drug concentration-time curves in the brain, a large number of animals are usually needed because brain tissue can only be sampled once in each animal. Furthermore, interanimal variability often complicates interpretation of the data.

Sierdal et al. [35] reported a brain/plasma MTX concentration ratio of 0.205 in rats. Intratumoral injection of radiolabeled MTX in mice results in a variable uptake of MTX in different areas of normal brain and brain tumor [38]. Jain et al. [23], in a series of studies in subcutaneous Walker 256-bearing rats, determined that MTX tumor-to-plasma concentration ratios are both time and dose dependent, and vary from approximately 0.7 to 5.0. Nierenberg et al. [28] reported greater MTX concentrations in and near brain tumor than in ventricular CSF or serum in adults. However, the analysis of brain tissue homogenates, as in these studies, neither provides a measure of total brain drug concentrations, nor allows distinction between extracellular and intracellular total and free drug concentrations. The disposition of anticancer drugs in brain tumors has not been studied by microdialysis. Therefore, the aims of this study were to (1) analyze the utility of the microdialysis technique in brain tumor-bearing rats and (2) compare brain extracellular concentrations and the pharmacokinetics of MTX in brain tumor-bearing and normal rats.

Materials and methods

Materials

MTX was donated by Lederle Laboratories (Pearl River, N.Y.). Lomotrexol (LT) was a gift from Eli Lilly Co. (Indianapolis, Ind.). The following chemicals were purchased from Sigma Chemical Co. (St. Louis, Mo.) and used as received: calcium chloride, sodium chloride, potassium chloride, potassium phosphate dibasic. CMA/12 microdialysis probes, guide cannulas, dialysis tubing and tubing connectors were purchased from Bioanalytical Systems (West Lafayette, Ind.). Anchor screws and a pin vise were purchased from Small Parts (Miami, Fl.). Methanol was purchased from J.T. Baker (Phillipsburg, N.J.). Male Fischer rats were obtained from Taconic Farms (Germantown, N.Y.).

Equipment

A rodent stereotaxic frame was purchased from Stoelting Physiology Research Instruments (Wood Dale, Ill.), and had attached a microinjector unit obtained from David Kopf Instruments (Tujunga, Calif.). A constant rate infusion pump was obtained from Harvard Apparatus (South Natick, Mass.). HPLC analyses of samples were performed with a Hewlett Packard Model 1050 liquid chromatographic system (Sunnyvale, Calif.).

RG-2 cell line

The rat glioma-2 (RG-2) cell line was used for all studies [44]. The cells were maintained in Dulbecco's minimum essential medium supplemented with 10% fetal calf serum. The cells were grown as a monolayer at 37 °C in a humidified atmosphere of 5% CO_2 and 95% air. For transplantation of cultured cells into the rat brain, exponential growth cultures were harvested by trypsinization (0.04% trypsin, 10 min), centrifuged and resuspended in Dulbecco's medium. The cells were counted in a hemocytometer, diluted to a concentration of 1×10^5 cells/10 µl and placed on ice until implantation, usually within hours.

Animal preparation

Male Fisher rats weighing 225–250 g were maintained on food and water *ad libtium* and were allowed to adapt to the animal housing environment for at least 1 week prior to the study. The rats were anesthetized with an intraperitoneal dose (0.1 ml/100 g body weight) of a 3:2:1 (v v v) mixture of ketamine hydrochloride (100 mg/ml), acepromazine maleate (10 mg/ml) and xylazine hydrochloride (20 mg/ml) and secured in the stereotaxic apparatus. The scalp was cleaned with 70% alcohol and the skull exposed by a midline scalp incision. Tissue covering the skull was gently everted and the bregma identified. A small burr hole was drilled at a position 2 mm posterior, and 2 mm lateral from the bregma and above the thalamic region. For calculation of the desired coordinates, reference was made to the atlas of Paxinos and Watson [30]. Two additional small holes were drilled for bone anchor screws several millimeters away from the burr hole. After inserting the bone anchor screws, 10 µl of the tumor cell suspension was slowly injected over 30–45 s into the right thalamic region at a depth of 4.5 mm. After a waiting period of 60 s, the needle was removed from the brain, and a guide cannula

was slowly lowered to a depth of 3 mm. Dental cement was used to anchor the guide cannula and the supporting screws. The incision was sutured to cover the cement, leaving only the cannula exposed. Animals used as control were treated exactly in a similar way to tumor rats, except RG-2 cells were not implanted.

Animals were then returned to their cages and received standard rat diet and water *ad libitum*. Once animals became symptomatic (i.e. 10–14 days after implantation) with lethargy, arched back and pigmentation of the eyelids, they were anesthetized with an intraperitoneal dose (0.03 ml/100 g body weight) of the same anesthetic preparation used previously. An incision just right of midline was made in the neck. The right common carotid artery, the external carotid artery and the right pterygopalatine artery were isolated and ligated. A small cut was made in the right common carotid artery, and a PE 50 cannula filled with sodium heparin (100 IU/ml) was inserted with the cannula tip near the bifurcation between the internal and external carotid arteries. The cannula was tied into place. For serial blood sampling, a PE 50 cannula filled with heparin (100 units/ml) was inserted into the right jugular vein. After the cannulas were placed, and exteriorized at the back of the neck, the incisions were sutured.

Dialysate preparation and probe calibration

Simulated CSF (pH 7.6) consisting of 1.1 m*M* magnesium chloride ($MgCl_2$), 1.35 m*M* calcium chloride ($CaCl_2.2H_2O$), 3 m*M* potassium chloride (KCl), 0.242 mM disodium hydrogen phosphate ($Na_2HPO_4.7H_2O$), 20 mM sodium bicarbonate ($NaHCO_3$) and 131.9 m*M* sodium chloride (NaCl) was prepared the day of the experiment. LT (calibrator) solution was prepared at a concentration of 1 μg/ml in simulated CSF solution at room temperature.

The previously inserted dummy cannula in the thalamic guide cannula was replaced by a 2-mm CMA/12 probe. A solution of LT (1 μg/ml) was perfused through the microdialysis probe using a Harvard infusion pump at a flow rate of 3 μl/min for at least 1 h prior to the administration of MTX.

Microdialysate and blood sampling

Freshly prepared MTX solution (50 mg/kg) in PBS (pH 8.0) was then administered over 1 min intraarterially, followed by 0.5 ml heparinized (100 units/ml) saline. After correction for dead volume, the dialysate was continuously collected into Ependorff vials every 20 min for 3 h. Blood samples (0.25 ml) were drawn into heparinized tubes at predetermined time-points after administration of the MTX dose, and centrifuged immediately to obtain plasma. The cannulas were filled with heparinized saline after each blood sampling. Plasma, and dialysate samples were then stored at $-80\,^{\circ}C$ until further analysed for MTX.

At the end of 3 h, five animals in the RG-2 group (out of eight animals) and three animals in the normal group (out of five animals) were killed by decapitation and the head with the microdialysis probe was fixed in formalin ($\sim$ 3 days). The whole brain was extracted, tissues adjacent to the probe were obtained, embedded in paraffin, sectioned, stained with hematoxylin and eosin (H & E) and examined by light microscopy to determine placement of the probe.

Methotrexate analyses

MTX concentrations in plasma were quantitated using an HPLC method. Briefly, 20 μl trichloroacetic acid was added to 150 μl plasma sample, vortexed and centrifuged at 10 000 rpm for 10 min. The supernatants were injected onto an HPLC system where separation was achieved on a Hypersil ODS column C_{18}(200 mm $\times$ 2.1 mm) using a mobile phase of 20% (v/v) methanol, 40 m*M* dibasic potassium phosphate, pH 7.0, delivered at a flow rate of 0.3 ml/min. UV detection was made at 280 nm. Assay precision between days was characterized by a coefficient of variation ranging from 3% to 17% over an MTX concentration range of 1 μg/ml and 30 μg/ml in plasma. MTX concentrations in dialysate were also determined by HPLC as described above, except dialysate samples were injected directly onto the HPLC system. The interday coefficient of variation ranged from 3.9% to 13.3% for dialysate concentrations ranging from 37.5 to 1000 ng/ml.

In vitro dialysis study

The microdialysis probe was immersed in a beaker containing MTX in simulated CSF (1.0 μg/ml). LT (1.0 μg/ml) prepared in simulated CSF was infused through the probe at a flow rate of 3 μl/min for 1 h and the dialysate was collected every 20 min for 2 h. MTX and LT concentrations in dialysate ($C_{dialysate}$) and reservoir samples ($C_{reservoir}$) were determined by HPLC as described above.

Data analysis

The method of retrodialysis utilizing a calibrator and the calculation of microdialysis recoveries in vitro and in vivo have been described previously [21, 43]. In vitro recovery of the probes was calculated using Eq. 1, the ratio of MTX concentrations in effluent dialysate to the probed reservoir:

$$\text{Recovery}_{\text{in vivo}} = \frac{C_{\text{dialysate}}}{C_{\text{reservoir}}} = \frac{\text{peak height of MTX}_{(\text{dialysate})}}{\text{peak height of MTX}_{(\text{reservoir})}} \quad (1)$$

The in vivo microdialysis recovery of MTX was estimated by the loss of calibrator LT relative to the reservoir concentration:

$$\text{Recovery}_{\text{in vivo}} = 1 - \left[\frac{\text{peak height of LT}_{\text{dialysate}}}{\text{peak height of LT}_{\text{reservoir}}}\right] \quad (2)$$

The mean in vitro and in vivo recoveries were calculated and compared. Concentrations of MTX in the dialysates from the thalamus were then corrected by the in vivo recovery to obtain the corresponding concentrations in thalamus ECF over the dialysate collection interval.

Polyexponential equations were fitted to the plasma and interstitial concentration-time data:

$$C_i = \sum_{i=1}^{n} A_i \exp(-\lambda_i t) \quad (3)$$

where C_i is the concentration of MTX in the plasma or interstitial fluid (i), λ_i are the apparent first-order disposition rate constants, and Ai are the corresponding zero-time intercepts. The best-fit form of Eq. 3 was assessed by Akaike's information criterion [31]. Area under the curve in brain interstitial region (AUC_b), area under the curve in plasma (AUC_p), area under the first moment curve (AUMC), and mean residence time (MRT) in the plasma were computed from the following equations:

$$AUC_i = \sum_{i=1}^{n} A_i/\lambda_i \quad (4)$$

$$AUMC_p = \sum_{i=1}^{n} A_i/\lambda_i^2 \quad (5)$$

$$MRT_p = AUMC_p/AUC_p \quad (6)$$

$$CL_T = \text{dose}/AUC_p \quad (7)$$

$$V_{ss} = (MRT_p \times \text{dose})/AUC_p \quad (8)$$

where CL_T is the total clearance and V_{ss} is the volume of distribution at steady state. The subscript i denotes plasma or interstitial fluid. A two-way ANOVA was used to compare differences between brain tumor-bearing and normal rats. A probability value of less than 0.05 was considered statistically significant. A hybrid physiologically based pharmacokinetic model was developed to characterize the brain interstitial fluid MTX concentration in both normal and RG-2 animals (see Appendix).

Results

The in vitro recovery of MTX from the probe was $12 \pm 3\%$. The recovery of MTX from the thalamus probe in vivo, calculated from the in vivo loss of LT was $10 \pm 4\%$.

The mean plasma concentration time curves for MTX in RG-2 glioma-bearing and normal rats is shown in Fig. 1. Each point represents the average value obtained from five to eight rats. The plasma concentrations of MTX declined biexponentially. This was in concordance with the findings of Bremnes et al. [7] who reported biphasic plasma elimination of MTX after intravenous injections of 10–1000 mg/kg in rats. However, despite equivalent doses of MTX, plasma MTX concentrations in tumor-bearing animals were found to be greater than those obtained in control animals. Table 1 compares the MTX pharmacokinetic parameters in tumor-bearing and normal rats. CL_T and V_{ss} varied from 0.90 ± 0.37 to $0.24 \pm 0.02\ l h^{-1} kg^{-1}$ and from 0.58 ± 0.24 to $0.2 \pm 0.16\ l\ kg^{-1}$, respectively, with normal and tumor-bearing rats. The mean terminal half-life of MTX was significantly increased from 37.61 min (normal rats) to 76.62 min (tumor-bearing rats).

Figure 2 show the mean concentrations of MTX in brain ECF vs time in RG-2 glioma-bearing rats and normal rats, respectively. ECF MTX concentrations were corrected for the in vivo recovery as described above and represent time-averaged concentrations over 20-min intervals. Brain ECF MTX concentrations in both normal and RG-2 rats declined in parallel with plasma concentrations, and were significantly greater in the RG-2 animals. Table 2 summarizes

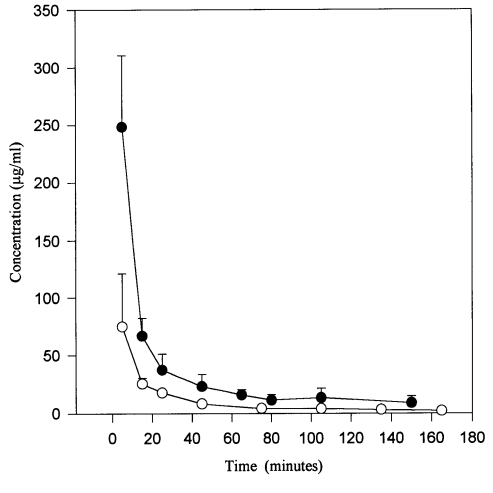

Fig. 1 Methotrexate plasma concentration-time profiles in (●) RG-2 glioma-bearing and (○) normal rats following an intraarterial dose of 50 mg/kg. Each point represents the mean ± SD from a minimum of five rats in the RG-2 group and three rats in the normal group

Table 1 Pharmacokinetic parameters for methotrexate in RG-2 glioma-bearing bearing and normal rats following an intraarterial dose of 50 mg/kg. ($n = 8$ RG-2 group, $n = 5$ normal group). All values are means ± SD

Pharmacokinetic parameter	RG-2 rat	Normal rat
$CL_{(T)}$ ($l\ h^{-1}\ kg^{-1}$)	0.244 ± 0.022*	0.899 ± 0.372
V_{ss} ($l\ kg^{-1}$)	0.214 ± 0.159*	0.575 ± 0.241
$t_{1/2}$ (min)	76.62 ± 29.23	37.61 ± 12.87
MRT (min)	59.66 ± 43.93	32.77 ± 12.05

* $P < 0.05$ vs normal rat

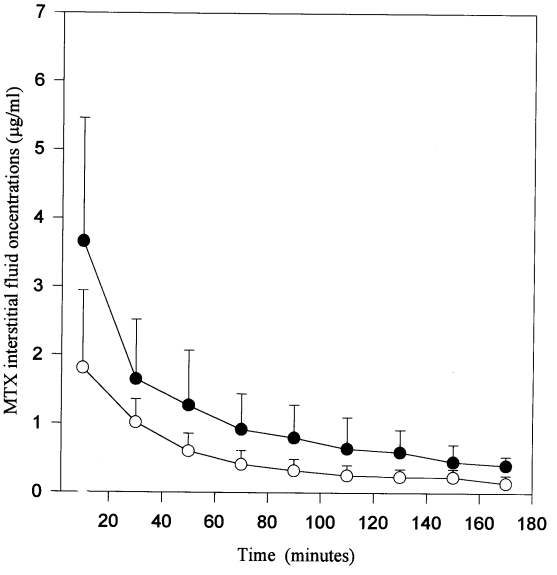

Fig. 2 Methotrexate concentration-time profiles in brain interstitial fluid of (○) normal and (●) RG-2 glioma-bearing rats following an intraarterial dose of 50 mg/kg. Each point represents the mean ± SD ($n = 8$ RG-2 group, $n = 5$ normal group)

Table 2 Area under the methotrexate concentration time curve in plasma (AUC_p) and brain extracellular fluid (AUC_b), and ratio in control and tumor-bearing rats following an intraarterial dose of 50 mg/kg ($n = 8$ RG-2 group, $n = 5$ normal group) All values are means ± SD

	RG-2 rat	Normal rat
AUC_p (µg-min/ml)	12419.6 ± 1334.5*	4100.7 ± 2516
AUC_b (µg-min/ml)	583.5 ± 296.7*	171.59 ± 69.14
AUC_p/AUC_p	0.047 ± 0.022	0.051 ± 0.032

* $P < 0.05$ vs normal rat

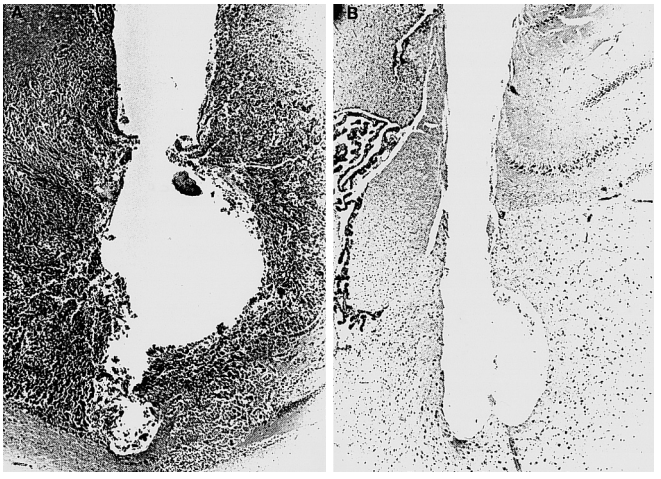

Fig. 3 a,b Photomicrographs of brain from RG-2 glioma-bearing and normal rats showing microdialysis probe in the (**a**) brain tumor and (**b**) normal brain (H&E stain, × 50)

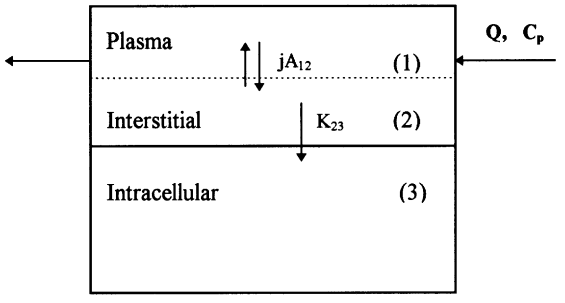

Fig. 4 Pharmacokinetic model of MTX in rat brain. See Appendix for definition of symbols

the AUC values for MTX plasma (AUC_p) and brain ECF (AUC_b). In this study, the AUC_b/AUC_p ratios were found to be approximately 0.051 ± 0.032 and 0.047 ± 0.022, for control and tumor-bearing rats and were not significantly different ($P > 0.05$). The $(AUC_b)_{RG-2}/(AUC_b)_N$ was approximately 3.2 and may be a result of enhanced blood–tumor barrier (BTB) permeability or elevated plasma MTX concentrations in the RG-2 group.

Microscopic analyses on brain sections adjacent to the microdialysis probe were done to verify the exact placement of the probe. Representative examples are shown in Fig. 3. On microscopic examination of the brain tumor tissue (Fig. 3a) a narrow elongated space produced by the passage of the probe and projecting into the area of the tumor was seen.

Figure 4 illustrates a physiologically based pharmacokinetic model for MTX in brain. Observed and model-predicted MTX concentrations are shown in Fig. 5 and 6 for normal and RG-2 rats. The model predicted interstitial MTX concentration data well

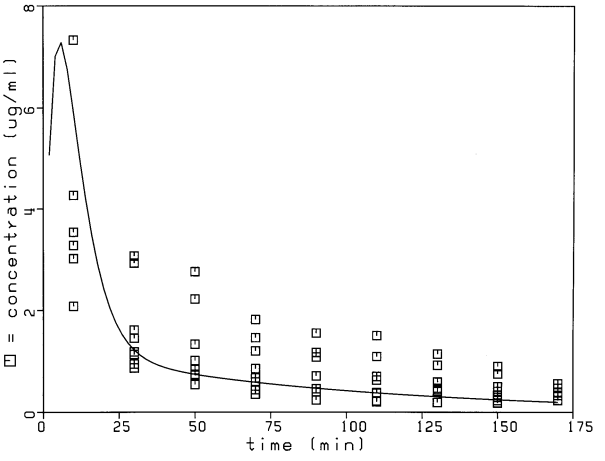

Fig. 5 Observed (□) and hybrid physiologically based pharmacokinetic model-predicted (solid line) MTX concentration in RG-2 glioma-bearing rats following an intraarterial dose of 50 mg/kg

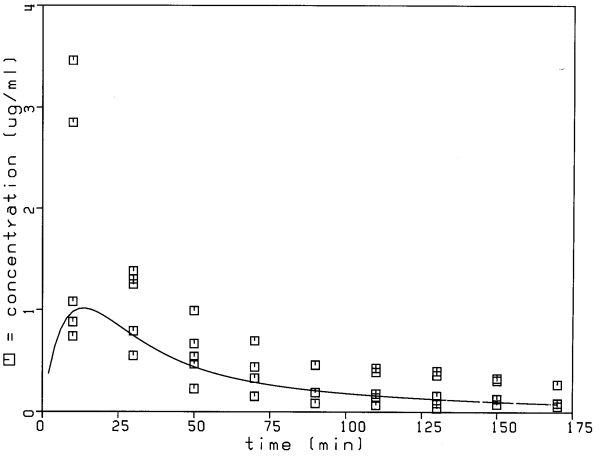

Fig. 6 Observed (□) and hybrid physiologically based pharmacokinetic model-predicted (solid line) MTX concentration in normal rats following an intraarterial dose of 50 mg/kg

with few exceptions. The model parameters are listed in Table 3. BBB transport, indicated by h_{12}, in tumor was twofold higher than that for control, consistent with enhanced capillary permeability and BBB breakdown.

Discussion

Caffeine has been utilized as a retrodialysis calibrator in the microdialysis of theophylline in rat brain [25]. Wong et al. [46] reported the use of 3′-azido-2′,3′-dideoxyuridine during retrodialysis of azidothymidine (AZT) in rabbit brain. In this study, LT, an analog of MTX, was used as a retrodialysis calibrator (see Fig. 7).

Table 3 Parameters used in hybrid physiologically based pharmacokinetic model of methotrexate in the rat

Parameter	RG-2 rat	Normal rat
Forcing function parameters		
A_1 (μg/ml)	511.65	130.25
A_2 (μg/ml)	38.10	21.81
λ_1 (min^{-1})	0.176	0.172
λ_2 (min^{-1})	0.011	0.018
Physiological parameters		
Q (ml/min)	0.27	0.32
V (ml)	0.2937	0.2937
V_1 (ml)	0.0067	0.0011
V_2 (ml)	0.098	0.1004
fu_1	0.62	0.62
fu_2	1.0	1.0
Transport parameters		
h_{12} (ml/min)	8.9×10^{-4}	2.75×10^{-4}
K_{23} (ml/min)	0.266	0.0052

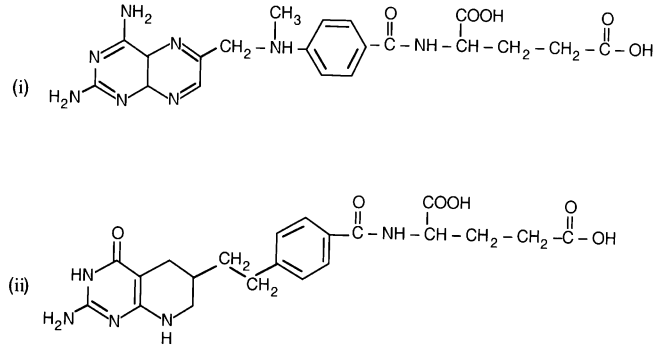

Fig. 7 Structures of (i) methotrexate and (ii) lomotrexol

According to Groothuis et al. [18] an animal brain tumor model should exhibit the following criteria: (1) the tumor should originally be a brain tumor, and (2) the tumor production rate, growth and histological grading should be predictable and reproducible. The RG-2 brain tumor model used in this study fulfilled these criteria, and has been previously used in pharmacokinetic studies [14]. Following tumor implantation and recovery from anesthesia, the animals rapidly resumed normal activity without showing ill effects. After a 2-day period of postoperative weight loss, the animals gained weight temporarily. A second period of weight loss was among the first signs of clinical deterioration, and consisted of approximately 25% loss of body weight over the 2-week study period. In addition, there was a progressive decline in functional activity. At 11–13 days, most animals exhibited ruffled coats, a lack of grooming and periorbital hemorrhage.

The brain tissue reactions to the implantation of microdialysis probes have been investigated. Implantation of microdialysis probes has been shown not to compromise the integrity of the BBB, as evidenced by the recovery of $< 0.2\%$ of sodium technetate (which is unable to penetrate intact BBB) during 80 min of dialysis after probe implantation into the rat brain.

Pharmacokinetic studies of MTX in rats have revealed both biexponential and triexponential concentration-time profiles in plasma [8]. Fahrig et al. [16] have shown that MTX is not appreciably metabolized in rats, and thus the concentration profile indicates rapid localization in tissues combined with biliary and renal excretion. Bremnes et al. [7] reported a biphasic plasma elimination of MTX after intravenous injections of 10–1000 mg/kg in rats. Following intraarterial injection of MTX, the plasma concentrations decreased very rapidly for a few minutes, followed by a longer exponential phase. The reduction in CL_T and V_{ss} in tumor-bearing rats may reflect cachexia and volume depletion in these animals. Malnutrition and the presence of a tumor influence the host's metabolic state [39], so the animals, may have had altered hepatic enzyme activity and prolonged enterohepatic circulation of MTX. MTX is excreted into the urine through an active tubular secretion (ATS) mechanism, and accounts for 48% of elimination in rats [16]. Since ATS is energy dependent, its efficacy and accordingly CL_T, may have been reduced in tumor-bearing rats. The reduction of V_{ss} in tumor-bearing rats may be attributed to a reduction in total body water, as well as a change in protein binding. A reduction in the number of protein binding sites through a reduction in protein synthesis in the tumor-bearing rats may have led to saturation of tissue protein binding. Such a reduction in MTX binding to tissue proteins, as opposed to plasma proteins, would result in an increased fraction unbound in tissues, and accordingly a reduction in the V_{ss} [45].

Since the tumor cells were injected at a depth of 4.5 mm, the microdialysis probe with a 2-mm dialysis membrane and placed at a depth of 3 mm, would overlap the site of tumor cell injection ventrally. Other coordinate relations between the tumor cell innoculation site and placement of the guide cannula may have also resulted in collection of ECF from the tumor. However, even if the probe is outside the tumor it can still provide meaningful data on drug uptake in brain. By knowing the location of the probe in relation to the tumor, the interstitial fluid drug concentration data can be interpreted accordingly. Sampling just beyond the outer edge of the tumor, the so-called brain surrounding tumor region, may show intermediate permeability compared to interstitial fluid samples obtained at the tumor periphery and necrotic core. In fact, interanimal variability in interstitial fluid drug concentrations may be an indication of anatomic differences in sampling sites. The variability in interstitial fluid MTX concentrations (see Table 2, AUC_b) was somewhat greater in the tumor-bearing group than in the normal group, and thus could have resulted from different anatomic sampling sites within the tumor. Photomicrographs for

all tumor animals were similar in terms of the density of tumor cells surrounding the probe.

Jain et al. [23] had previously measured subcutaneous tumor (i.e. H5123 and W256) and normal MTX interstitial fluid concentrations using a micropore diffusion chamber. MTX interstitial fluid concentrations were generally less than those measured in plasma and in tumor (total homogenate), and were similar in tumor and normal interstitial fluid. The AUC_b/AUC_p ratio (see Table 2), being about 0.05 in both control and brain tumor-bearing rats was approximately tenfold lower than MTX concentration ratios based on total brain homogenates or CSF [23] (see Introduction). Barnett et al. [2] characterized differential permeability of MTX in an intracerebral human LX-1 small-cell lung carcinoma xenograft model and reported that the PS product (capillary permeability, P, $\times$ capillary surface area, S) was approximately nine times higher in subcutaneous tumor than in the intracerebral tumor 8 days after tumor inoculation. Therefore, the comparisons between intracerebral tumor and subcutaneous tumor must be guarded because of differences such as blood flow, permeability, and size [2]. It would have been of interest to obtain total brain MTX concentrations in the current investigations for comparative purposes, but all brains were processed for probe localization (Fig. 3).

An interesting unresolved issue is the basis for the higher MTX ECF concentrations in the RG-2 group than in the normal group. Are these higher values the result of BBB breakdown or, in light of the near equivalent AUC_b/AUC_p, a function of high plasma MTX concentrations in the presence of a normal BBB? A model that accounted for both BBB transport and elevated plasma MTX concentrations was developed to further explore these phenomena and their contribution to the ECF MTX concentrations.

The model (see Fig. 4) incorporates linear BBB or BTB transport processes, and also a unidirectional interstitial to intracellular (K_{23}) clearance. This model was able to predict ECF MTX concentrations in both the normal and tumor-bearing animals. Based on the work of Dedrick et al. [12], MTX disposition in normal tissues shows saturable transport and is influenced by strong intracellular binding. Other reasonable models include nonlinear transport from plasma into interstitial fluid, bidirectional interstitial–intracellular transport as well as saturable binding in the intracellular compartment. These alternative models did not adequately describe the data.

The h_{12} values obtained for normal (2.75×10^{-4} ml/min) and RG-2 animals (8.9×10^{-4} ml/min) in the current model were within the range of values obtained by Barnett et al. for MTX in a human lung carcinoma brain xenograft model [2]. This model clearly demonstrates that the higher ECF MTX concentrations in RG-2 animals are partially a function of a more permeable BBB (see h_{12} values). The higher plasma MTX concentrations, accounted for in the forcing function, in RG-2 animals do not solely explain the high ECF MTX concentrations. Assumption of equivalent BBB permeability in RG-2 animals to that in normal animals resulted in an overprediction of the observed AUC_b. Marker substances such as aminoisobutyric acid (AIB) [17], do show enhanced BBB or BTB permeability in experimental models for brain tumors and thus, increased permeability of MTX at the BTB is consistent with these observations. Higher permeability in tumor capillaries is also consistent with ultrastructural observations that tumor capillaries have wider interendothelial gaps and a less continuous basement membrane than capillaries in normal brain.

The model has assumed unidirectional MTX transport from the interstitial space to the intracellular compartment. As stated above, alternate models that consider bidirectional transport did not adequately characterize the data. The model, thus presumes that the counter-flux of MTX from the intracellular to the interstitial compartment is negligible over the time-frame of the experiment. This negligible counter-flux of MTX may be attributed to appreciable intracellular binding and metabolism of MTX, including MTX polyglutamates which do not readily exit cells. It is also noted that the unidirectional clearance (see K_{23}, Table 3) was greater in RG-2 animals than in normal animals, and thus MTX's uptake into tumor cells is more appreciable than into normal brain parenchyma cells. No direct evidence of MTX's intracellular uptake, binding or metabolism were obtained in the current investigation. However, the model assumptions pertaining to these phenomena have reduced the complexity of the model that is consistent with the experimental data.

In conclusion, the microdialysis technique was successfully utilized to examine the extracellular distribution of MTX in brain of normal and glioma-bearing rats. It was shown that higher free MTX ECF concentrations in tumor animals is partly attributed to a more permeable BBB. The microdialysis method will be useful to examine anticancer drug disposition in the tumor compartment and facilitate an understanding of factors that influence drug uptake. The potential uneven distribution of drugs within solid tumors due to heterogeneities in tumor blood flow and permeability [23] can be specifically analyzed with microdialysis. In particular, two probes placed in or near the tumor can provide simultaneous measurements of ECF drug concentrations that result from differences in the microenvironment. Beyond characterization of a drug's intratumoral kinetics, measurement of tumor ECF drug concentrations will enable a variety of experimental therapeutic drug regimens to be evaluated. Targeted drug delivery, combination drug regimens, such as with a modulator of drug resistance, and cellular pharmacodynamic strategies may be efficiently addressed with microdialysis techniques.

Appendix

Model development

Transport of MTX into Lewis lung tumor tissue [47] and several normal tissues [12] in rats has been described, in which the uptake rate is limited by the membrane permeability. The principles of these models have formed the basis to investigate a model for MTX in rats bearing RG-2 gliomas. However, certain assumptions were deemed necessary (see below) that required fewer model parameters than used previously in other animal models. Thus, our approach was to develop as simple a model as possible, including the predominant processes governing MTX transport, that was able to analyze the experimental data.The following model assumptions were made: (1) only unbound MTX can distribute between plasma and brain, (2) binding of MTX to plasma proteins is linear and equal for both normal and RG-2 groups, (3) no MTX binding occurs in the interstitial compartment, (4) membrane transport is first-order and (5) MTX intracellular clearance is irreversible. Consistent with these assumptions were the following mass balance equations:

$$V_1 \frac{dC_{1f}}{dt} = fu_1 \left[Q \left(C_p - \frac{C_{1f}}{fu_1} \right) - jA_{12} \right] \quad \text{(A 1)}$$

$$jA_{12} = h_{12}(C_{1f} - C_{2f}) \quad \text{(A 2)}$$

$$V_2 \frac{dC_{2f}}{dt} = fu_2[jA_{12} - K_{23}C_{2f}/fu_2] \quad \text{(A 3)}$$

where Q is the blood flow rate, C_f is the free MTX concentration, jA is the net transport rate of MTX over total area A, V1 is the capillary volume, V_2 is the interstitial volume, h_{12} is the mass transfer coefficient across the BBB, K_{23} is the interstitial to intracellular clearance parameter, fu_1 and fu_2 refer to the fraction unbound in plasma and interstitial fluid, respectively. The subscripts 1, 2, 3 and p refer to vascular, interstitial, intracellular, and plasma, respectively.

The term C_p was set equal to a forcing function obtained by fitting polyexponential equations to all the MTX plasma data within the RG-2 and normal groups. Each group was best described by a biexponential equation of the form:

$$C_p = A_1 e^{(-\lambda_1 t)} + A_2 e^{(-\lambda_2 t)} \quad \text{(A 4)}$$

where λ_1, and λ_2 are the apparent first-order fast and slow disposition rate constants, respectively, and A_1, A_2, are the corresponding zero-time intercepts.

Organ blood flows [13], total tissue volumes and subcompartment volumes (capillary, interstitial and intracellular) [5] were obtained from the literature and adjusted to the total body weight of 225 g. These along with fraction unbound in plasma and interstitial fluid (fu_1 and fu_2) were treated as constants. Equations A1–A3 were solved by numerical integration that utilized a maximal likelihood optimization method to estimate h_{12} and K_{23} based on all the ECF MTX data (i.e., C_{2f}) for each group. The computer program SimuSolv [36] was used for model development.

Acknowledgement This project was supported in part by NIH grant NS34634.

References

1. Allen JC, Walker R, Rosen G (1988) Preradiation high-dose intravenous methotrexate with leucovorin rescue for untreated primary childhood brain tumors. J Clin Oncol 6:649–653
2. Barnett PA, Roman-Goldstein S, Ramsey F, McCormick CI, Sexton G, Szumowski J, Neuwelt EA (1995) Differential permeability and quantitative MR imaging of a human lung carcinoma brain xenograft in the nude rat. Am J Pathol 146:436–449
3. Ben-Nun J, Cooper JR, Cringle SJ, Constable IJ (1988) Ocular dialysis. A new technique for in vivo intraocular pharmacokinetic measurements. Arch Opthalmol 106:254–259
4. Benveniste H (1989) Short review: brain dialysis. J Neurochem 52:1667–1679
5. Bischoff KB, Brown RG (1966) Drug distribution in mammals. Chem Eng Prog Symp 62:33–45
6. Bito L, Davson H, Murray LM, Snider N (1966) The concentrations of free amino acids and other electrolytes in cerebrospinal fluid, in vivo dialysate of brain, and blood plasma of dog. J Neurochem 13:1056–1067
7. Bremnes RM, Slordal L, Wist E, Aarbakke J (1989) Dose-dependent pharmacokinetics of methotrexte and 7-hydroxy-methotrexate in the rat in vivo. Cancer Res 49:6359–6364
8. Bremnes RM, Slordal L, Wist E, Aarbakke J (1989) Formation and elimination of 7-hydroxy-methotrexate in the rat in vivo after methotrexate administration. Cancer Res 49:2460–2464
9. Brooks DJ, Beaney RP, Lammerstama AA, Herold S, Turton DR, Luthra SK, Frackowiak AS, Thomas DG, Marshall J, Jones T (1986) Glucose transport across the blood-brain barrier in normal human subjects and patients with cerebral tumors studies using [^{11}C]-3-O-methyl-D-glucose and positron emission tomography. J Cereb Blood Flow Metab 6:230–239
10. Candler KL, Prados MD (1994) Chemotherapy of brain tumors: clinical aspects. In Morantz RA, Walsh JW (eds) Brain tumors: a comprehensive text. Marcel Dekker, New York, pp 731–734
11. Chatelu E, Roche H, Plusquellec Y, Peyrille F, Deßiasi J, Pujol A, Canal P, Houing (1991) Pharmacokinetic modeling of plasma and cerebrospinal fluid methotrexate after high-dose intravenous infusion in children. J Pharm Sci 80:730–734
12. Dedrick RL, Zaharko DS, Lutz RJ (1973) Transport and binding of methotrexate in vivo. J Pharm Sci 62:882–890
13. Delp MD, Manning RO, Bruckner JV, Armstrong RB (1991) Distribution of cardiac output during diurnal changes of activity in rats. Am J Physiol 261:H1487- H1493
14. Devineni D, Klein-Szanto A, Gallo JM (1995) Tissue distribution of methotrexate following administration as a solution and as a magnetic microsphere conjugate in rats bearing brain tumors. J Neuro Oncol 24:143–152
15. Djerassi I, Kim JS, Kassarov L, Regev A, Gandhi V, Srivastava B (1988) High dose methotrexate with citrovorum factor in astrocytoma. Proc Am Soc Clin Oncol 7:82
16. Fahrig L, Brasch H, Iven H (1989) Pharmacokinetics of methotrexate and 7-hydroxymethotrexate in rats and evidence for metabolism of methotrexate to 7-hydroxymethotrexate. Cancer Chemother Pharmacol 23:156–160
17. Fross RD, Warnke PC Groothius DR (1991) Blood flow and blood-to-tissue transport in 9L gliosarcomas:the role of the brain tumor model in drug delivery research. J Neuro-Oncol 11:185–197
18. Groothuis DR, Fischer JM, Pasternak JF, Blasberg RG, Vick NA, Bigner DD (1983) Regional measurements of blood-to-tissue transport in experimental Rg–Z rat gliomas. Cancer Res 43:3368–3373
19. Hawkins RA, Phelps ME, Huang SC, Wapenski JA, Grimm PD, Parker RG, Juillard G, Greenberg P (1984) A kinetic evaluation of blood-brain barrier permeability in human brain tumors with ^{68}Ga-EDTA and positron computed tomography. J Cereb Blood Flow Metab 4:507–515
20. Herrera AM, Scott DO, Lunte CE (1990) Microdialysis sampling for determination of plasma protein binding of drugs. Pharm Res 7:1077–1081
21. Jacobson I, Sanderg M, Hamberger A (1985) Mass transfer in brain dialysis devices: a method for the estimation of extracellular amino acids concentration. J Neurosci Methods 15:263–268
22. Jain RK (1989) Delivery of novel therapeutic agents in tumors: physiological barriers and strategies. J Natl Cancer Inst 81:570–576

23. Jain RK, Wei J, Gullino PM (1979) Pharmacokinetics of methotrexate in solid tumors. J Pharmacokinet Biopharm 7:181–194
24. Kendrick KM (1989) Use of microdialysis in neuroendocrinology. Methods Enzymol 168:182–197
25. Larsson CI (1991) The use of an "internal standard" for control of the recovery in microdialysis. Life Sci 49:PL73-78
26. Lonnroth P, Jansson PA, Smith U (1987) A microdialysis method allowing characterization of intercellular water space in humans. Am J Physiol 253:E228-231
27. Morrison PF, Bungay PM, Hsiao JK, Ball BA, Mefford IN, Dedrick RL (1991) Quantitative microdialysis: analysis of transients and application to pharmacokinetics in brain. J Neurochem 57:103–119
28. Nierenberg D, Harbaugh R, Herbert Mauer L, Reeder T, Scott G, Fratkin J, Newman E (1991) Continuous intratumoral infusion of methotrexate for recurrent glioblastama: a pilot study. Neurosurgery 28:752–761
29. Palsmeier RK, Lunte CE (1994) Microdialysis sampling in tumor and muscle: study of the disposition of 3-amino-1,2,4-benzotriazine-1,4-di-N-oxide (SR 4233). Life Sci 55:815–825
30. Paxinos G, Watson C (1986) The rat brain in stereotaxic coordinates. Academic Press, San Diego, CA
31. RSTRIP, MicroMath Scientific Software, Salt Lake City
32. Sabol KE, Freed CR (1988) Brain acetaminophen measurement by in vivo dialysis, in vivo electrochemistry and tissue assay: a study of the dialysis technique in the rat. J Neurosci Methods 24:163–168
33. Scott DO, Sorenson LR, Steele KL, Puckett DL, Lunte CE (1991) In vivo microdialysis sampling for pharmacokinetic investigations. Pharm Res 8:389–392
34. Shapiro WR, Young DF, Mehta BM (1975) Methotrexate distribution in cerebrospinal fluid after intravenous, ventricular and lumbar injections. N Eng J Med 293:161–166
35. Sierdal L, Jager R, Kjave J, Aarbakke J (1988) Pharmacokinetics of 7-hydroxy methotrexate and methotrexate in the rat. Pharmacol Toxicol 63:81–84
36. SIMUSOLV Dow Chemical Co., Midland, Mich.
37. Stahle L, Segersvard S, Ungerstedt U (1990) Theophylline concentraion in the extracellular space of the rat brain: measurement by microdialysis and relation to behavior. Eur J Pharmacol 185:187–193
38. Tator CH, Wassenaar W (1977) Intraneoplastic injection of methotrexate for experimental brain-tumor chemotherapy. J Neurosurg 46:165–174
39. Torosian MH, Daly JM (1986) Nutritional support in the cancer-bearing host. Effects on host and tumor. Cancer 58: 1915–1929
40. Ungerstedt U, Hallstrom A (1987) In vivo microdialysis – a new approach to the analysis of neurotransmitters in the brain. Life Sci 41:861–864
41. Ungerstedt U, Pycock C (1974) Functional correlates of dopamine neurotransmission. Bull Schweiz Akad Med Wiss 1278:1–13
42. Wan SH, Huffman DH, Azarnoff DL, Stephens R, Hoogstraten B (1974) Effect of route of administration and effusions on methotrexate pharmacokinetics. Cancer Res 34:3487–3491
43. Wang Y, Wong SL, Sawchuk RJ (1993) Microdialysis calibration using retrodialysis and zero-net flux: application to a study of the distribution of zidovudine to rabbit cerebrospinal fluid and thalamus. Pharm Res 10:1411–1419
44. Wechsler W, Kleihaus P, Matsumoto S, Zulch KJ, Ivankovic S, Preussmann R, Druckney H (1969) Pathology of experimental neurogenic tumors chemically induced during prenatal and postnatal life. Ann N Y Acad Sci 159:360–408
45. Wilkinson R (1983) Plasma and tissue binding consideration in drug disposition. Drug Metab Rev 14:427–465
46. Wong SL, Wang Y, Sawchuk RJ (1992) Analysis of zidovudine distribution to specific regions in rabbit brain using microdialysis. Pharm Res 9:332–338
47. Yang KH, Fung WP, Lutz RJ, Dedrick RL, Zaharko DS (1979) In vivo methotrexate transport in murine lewis lung tumor. J Pharm Sci 68:941–945
48. Yokel RA, Allen DD, Burgio DE, McNamara PJ (1992) Antipyrine as a dialyzable reference to correct differences in efficiency among and within sampling devices during in vivo microdialysis. J Pharmacol Toxicol Methods 27:135–142